2005

An Acoustic Fluid-structure Simulation of a Theraputic Ultrasound Wire Waveguide Apparatus

Graham Gavin
Technological University Dublin, graham.gavin@tudublin.ie

M.S. Hashmi
Dublin City University

Finbar Dolan
Medtronic Vascular

See next page for additional authors

Recommended Citation

Gavin, G., Hashmi, M., Dolan, F., McGuinness, G.: An Acoustic Fluid-structure Simulation of a Theraputic Ultrasound Wire Waveguide Apparatus. Proceedings of the 2nd International Conference on Computational Bioengineering, DIT, 2005. doi:10.21427/zex5-7116

2005-01-01

An acoustic fluid-structure simulation of a theraputic ultrasound wire waveguide apparatus

Graham P. Gavin
Dublin Institute of Technology, graham.gavin@dit.ie

M.S J. Hashmi
Dublin City University

Finbar Dolan
Medtronic Vascular

Garrett B. McGuinness
Dublin City University

II INTERNATIONAL CONFERENCE ON COMPUTATIONAL BIOENGINEERING
H. Rodrigues *et al.* (Eds.)
Lisbon, Portugal, September 14-16, 2005

AN ACOUSTIC FLUID-STRUCTURE SIMULATION OF A THERAPEUTIC ULTRASOUND WIRE WAVEGUIDE APPARATUS

Graham P. Gavin*, M.S.J. Hashmi*, Finbar Dolan and Garrett B. McGuinness***

* School of Mechanical and Manufacturing Engineering, Dublin City University, Ireland
e-mail: graham.gavin@dcu.ie
e-mail: garrett.mcguinness@dcu.ie

** Medtronic Vascular Ltd., Galway, Ireland
e-mail: finbar.dolan@medtronic.com

Keywords: Ultrasound, Waveguide, Angioplasty, Acoustic, Fluid-Structure, Atherosclerosis.

Abstract. *The use of high-power low-frequency ultrasound transmitted down small diameter wire waveguides is an emerging technology that may have potential in the treatment of complicated atherosclerotic plaques in cardiovascular surgery. This form of energy delivery results in vibrating the distal-tip of the wire waveguide disrupting material by means of direct contact ablation and also cavitation, pressure waves and acoustic streaming in the surrounding fluid. This work describes a numerical acoustic fluid-structure model of the ultrasound wire waveguide and blood surrounding the distal tip. The structural analysis of the model predicts the natural frequencies of the waveguide and shows the extent to which these are affected by the presence of the distal-tip geometry, the surrounding fluid and the length of wire waveguide. These results are validated against experimental results on a 23.5 kHz waveguide apparatus. The acoustic fluid results show the pressure field developed in the surrounding blood and predicts pressure conditions sufficient to cause cavitation in a region close to the distal-tip. These results compare favourably with experimental measurements reported in the literature. The model will prove a valuable design tool in the further development of this potential minimally invasive technology.*

1 INTRODUCTION

1.1 Coronary Heart Disease

Coronary heart disease, stroke and other diseases of the circulation have been shown to be the leading cause of death in Europe, accounting for nearly half of all deaths with a total of 1.5 million people dying annually in the European Union. These conditions are collectively known as cardiovascular disease (CVD) [1].

The World Health Organization has attempted to quantify the global magnitude of the disease and estimates that as many as 16.7 million deaths worldwide can be attributed to CVD each year [2]. By 2020 CVD will be the leading cause of death in the developing world with worldwide deaths totalling 25 million.

Coronary heart disease is a blockage of the coronary arteries and results in a reduction of blood flow volume to the heart muscle. These blockages can develop as gradual long term events such as atherosclerosis, an abnormal thickening of the arterial wall resulting in loss of blood supply downstream or can occur more rapidly by clotting or by the occurrence of a thromboembolism [3].

Blockages and atherosclerosis can also occur in the peripheral arteries. Peripheral thromboembolism is considered the most common cause of sudden arterial occlusion [4].

1.2 Present Interventional Procedures and Complications

The vast majority of atherosclerotic lesions are treated by minimally invasive dilation procedures such as balloon angioplasty or stent implantation. During these procedures a guidewire first crosses the blockage and acts as a guide rail for the balloon or stent delivery catheter [5].

Once in place the distal balloon is dilated, mechanically loading the plaque against the arterial wall, with the goal of permanently deforming the lesion and restoring lumen diameter and blood flow to near-normal parameters. Stents are permanent scaffolds that remain *in situ* and support the dilated vessel.

The success rates of these procedures, however, are largely determined by numerous factors. The ability of the guidewire to cross the lesion is critical and is the main determinant of success in 80% of cases [6]. Chronic total occlusions and thrombus events can cause near or total occlusion of the artery and can prevent guidewire access.

In addition, the mechanical properties of the plaque material vary greatly and mechanical testing including tensile, compression and failure properties all report the wide variation with plaque varying from soft lipid gruel to the more advanced fibrous and calcified plaques [7, 8, and 9].

These calcified plaques tend to be able to resist the mechanical load from the balloon dilation procedures and higher pressures have to be utilised in order to fracture this rigid material. These complications tend to severely reduce the success rates when treating calcified lesions with standard methods [10]. This is largely due to the fact that the present dilation

procedures are unable to induce selective injury and with higher pressures healthy arterial tissue in the region is damaged.

It therefore appears desirable to be able to target calcified or totally occluded lesions and selectively damage, ablate or otherwise disrupt this rigid plaque material as a stand-alone procedure or as a pre-treatment to allow for more successful standard procedures.

1.3 Therapeutic Ultrasound in the Treatment of Atherosclerotic Plaque

The use of high-power low-frequency ultrasound in medicine has been introduced for aortic valve de-calcification and also focused ultrasound in lithotripsy for the disintegration of kidney and gallstones [11]. These devices and procedures are based on the fact that ultrasound at the correct frequency and amplitude can disrupt inelastic rigid tissue while healthy elastic tissue in the locality can remain largely unaffected.

It was therefore hypothesised that this form of ultrasonic energy in cardiovascular surgery may have the potential to fracture or ablate calcified or fibrous tissue while the more distensible healthy arterial tissue remains unaffected. Work began initially in the 1970s when Sobbe et al. [12, cited in 11] used ultrasound delivered via a wire probe to disrupt clots in animals and during the later work attempted to refine the ultrasound delivery method [13 and 14].

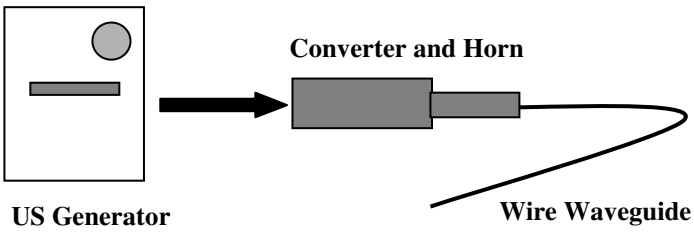

Figure 1: Schematic of Ultrasonic Waveguide Apparatus

Ultrasound (20-45 kHz) is generated external to the body by means of a piezoelectric converter and amplified by an acoustic horn. This results in the tip of the acoustic horn vibrating and acts as an input displacement (peak-to-peak) applied to and transmitted via a titanium alloy or aluminium alloy wire through the tortuous vascular structure to the lesion location as shown in Figure 1.

This form of energy manifests itself at the distal-tip of the wire waveguide as a large amplitude peak-to-peak displacement (0-150μm) at the driven ultrasonic frequency. The use of a spherical ball-tip or mushroom shaped tip is reported to increase drag and fluid motion around the distal tip [13 and 14]. Atar et al [15] suggest that disruption of the plaque material is due to four main mechanisms; direct contact ablation, cavitation, acoustic streaming and pressure wave components which are all directly related to distal-tip geometry, displacement and frequency.

Most work to date has concentrated on assessing the end clinical results of the delivery of therapeutic ultrasound and both Rosenschein et al [14] and Demer et al [16] reported favourable results when in vitro tests were performed on calcified atherosclerotic material. From these results and those reported by Siegel et al [17] it appears that ultrasonic energy delivered via small diameter wires is capable of disrupting fibrous and calcified plaques or total occlusions while avoiding damage to the adjacent healthy arterial tissue.

1.4 Present Work

This work focuses on the use of the numerical method to show how ultrasound energy is transmitted down a wire waveguide and how the resulting distal-tip displacements and geometry affect the pressure field developed in the surrounding fluid and the possibility of determining when cavitation occurs. This is critical, as non-contact ablation has been shown to only occur above the cavitation threshold [11].

Initially, the waveguide is to be modelled separately to assess its harmonic response in the absence of a distal ball-tip or other geometry and with no fluid present. This response will then be compared to a wire waveguide with ball-tip and also with a surrounding fluid to determine what affect, if any, these have of the performance of the waveguide. These structural results will be validated against the experimentally determined results for a wire waveguide apparatus operating at 23.5 kHz and transmitting via a 1.0mm nickel-titanium (NiTi) alloy described by Gavin et al [18].

Having determined the waveguide structural response the fluid results will be assessed to predict what affect distal-tip displacement and geometry have of the pressure field developed and will be compared to the experimentally determined pressure field plots reported in the literature by Makin et al [19] for a mushroom-tipped device operating at 22.5 kHz.

It is hoped this numerical model can address some of the mechanical design aspects of therapeutic ultrasound in the treatment of atherosclerotic plaques where little previous work appears in the literature and help in further refinement of this technology.

2 METHODS

2.1 Experimental Methodology

The ultrasonic waveguide apparatus (described in [18]) was used to transmit ultrasonic energy at 23.5 kHz down 1.0mm diameter NiTi wire waveguides. Peak-to-peak distal-tip displacements for various lengths of waveguide were experimentally determined by means of an optical microscope and image analysis software. Figure 2 shows an image obtained of the vibrating distal-tip and the superimposed peak-to-peak displacement determined by the image analysis software. Using this method we can also observe the achieved distal-tip displacements over a range of waveguide lengths and for various input displacements.

2.2 Numerical Analysis

In order to develop a model that could simulate both waveguide behaviour and acoustic fluid interaction at the distal-tip, firstly, a harmonic model of the waveguide was developed that could predict the steady-state response of the waveguide due to a sinusoidal input displacement. This represents the input the acoustic horn applies to the waveguide.

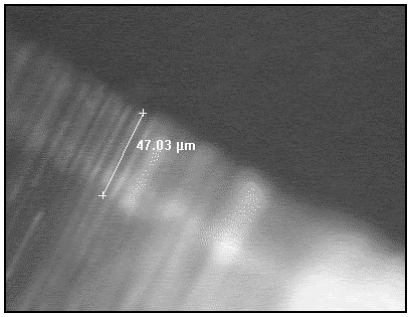

Figure 2: Image of the vibrating distal tip of the 1.0mm diameter wire waveguide

A 2D axisymmetric model of the waveguide was developed in ANSYS© using Plane42 structural elements. The problem sketch for the wire waveguide is shown in Figure 3. As mentioned the input to the model was a harmonic displacement while outputs included distal-tip displacements as a function of frequency or for a constant frequency the length of waveguide could be varied to see what affect this had on distal-tip displacement.

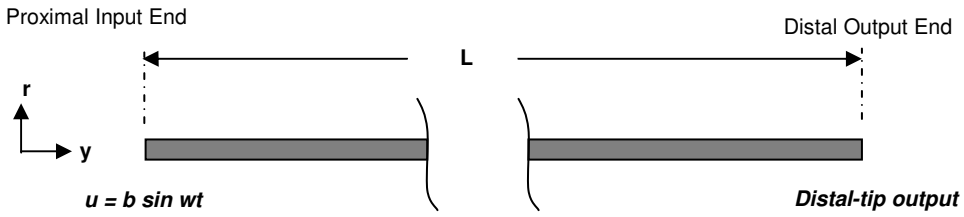

Figure 3: Problem sketch of wire waveguide

2.2.1 Mesh Density Modal Analysis

Initially a mesh density modal analysis was performed on the wire waveguide model to ensure that mesh density was sufficient to resolve all the resonant frequencies up to 30 kHz and subsequently accurately determine the internal wave structure and waveguide response at the frequencies of interest. The numerical modal results were compared against the analytical results [20] for the resonant frequencies (f) of a thin beam subjected to a sinusoidal input displacement given by:

$$f_n = \frac{nc}{4l} \qquad n = 1, 3, 5\ldots \tag{1}$$

where c is the speed of sound of the waveguide material and l is the length of the waveguide. Establishing confidence in these results allowed us to progress to a harmonic analysis.

2.2.2 Harmonic Analysis

A harmonic response analysis was performed on waveguides of multiple lengths and subjected to input displacements similar to those observed in the experimental testing of the waveguides. Both waveguides, with and without, distal tips were modelled.

From these simulations the overall steady-state response of the waveguide over a range of driven frequencies could be determined. This method was used to determine the affect the presence of a ball-tip has on the resonant frequencies of the waveguide. Also, for a fixed input frequency the distal-tip output of the wire waveguide for a range of lengths could be tested.

2.2.3 Harmonic Fluid-Structure Coupled Analysis

Having established the solid model could accurately the output distal-tip displacement of the waveguide and harmonic response, acoustic fluid elements Fluid29 and Fluid129 were included around the distal-tip. These elements allow for contact of fluid and structure and also the infinite acoustic boundary elements at a distance from the tip to allow no reflection of acoustic waves.

The inputs to this coupled acoustic fluid-structure model was the displacement input at a particular frequency to the proximal end of the wire waveguide while outputs included the distal tip displacements, natural frequencies and also the pressure field developed around the tip. Figure 4 shows the section of model around the distal tip of the waveguide with acoustic fluid elements.

Using this numerical approach an acoustic fluid structure model of a waveguide and distal-tip geometry described by Makin et al [20] was developed and the numerical pressure field results were compared with their experimentally determined pressures.

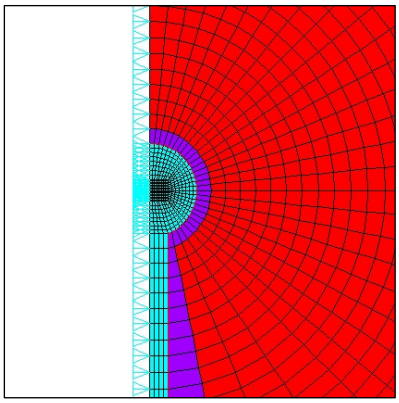

Figure 4: Axisymmetric FE model of distal-tip of wire waveguide in fluid

3 RESULTS AND DISCUSION

3.1 Structural Results

The results from the mesh density modal analysis are shown in Figure 5a and compared with the analytically determined natural frequencies in Table 1. Mesh density is defined as the number of elements in the radial direction (r) by the number of elements in the axial direction (y). The results show that an insufficient number of elements in the axial direction results in the higher natural frequencies being calculated incorrectly, higher than their correct value. This is further highlighted in the harmonic response of the waveguide shown in Figure 5b that shows the determined response for two mesh densities. The final mesh density chosen was sufficient to determine the harmonic response up to 30 kHz.

a)

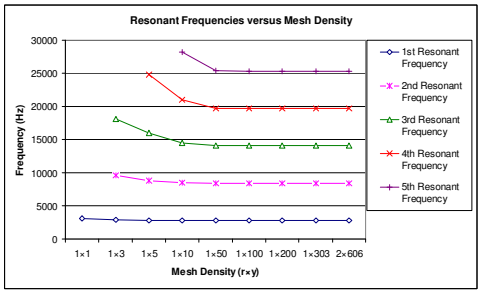

b)

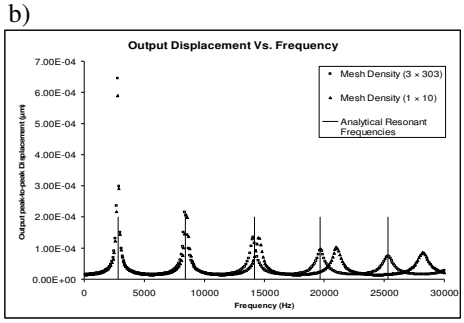

Figure 5: Results of mesh density modal and harmonic analysis for waveguide of l = 303mm.

Figure 6 shows the harmonic response of a 1mm diameter waveguide of 298mm length with and without a 2.6mm diameter ball-tip. The results show that the presence of the ball-tip has a moderate affect on the overall natural frequencies of the waveguide. This appears to be due to the fact that the mass and geometry of the ball-tip is small compared with the overall waveguide.

Analytical Resonant Frequencies (Hz)	**Numerical Resonant Frequencies (1 × 303) (Hz)**	**Percentage Error (%)**
2,840.83 (n=1)	*2,813.51*	*0.96*
8,438.11 (n=3)	*8,440.62*	*0.029*
14,204.16 (n=5)	*14,067.99*	*0.95*
19,688.94 (n=7)	*19,695.79*	*0.03*
25314.35(n=9)	*25,324.20*	*0.03*

Table 1: Comparison of analytical and numerical resonant frequencies for l = 303mm.

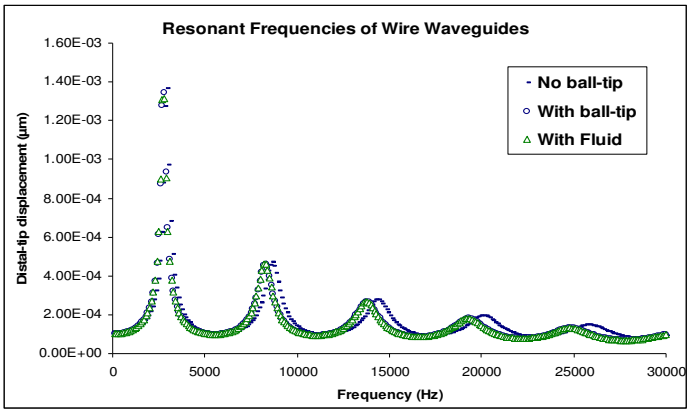

Figure 6: Numerically Determined Resonant Frequencies for waveguides

By modelling multiple lengths of waveguide and recording the distal-tip displacements at a fixed frequency of 23.5 kHz we can compare the numerical results of waveguide response to the experimentally results as shown in Figure 7. With the inclusion of a damping value of 4.5% (described in [18]) to account for all damping phenomena a good comparison is achieved.

These results show the critical relationship between the wire length and the distal-tip peak to peak displacement as the wire moves in and out of resonant lengths. These results also

compare favourably with the analytically determined non-resonant lengths for multiple waveguides at 23.5 kHz as shown in Table 2.

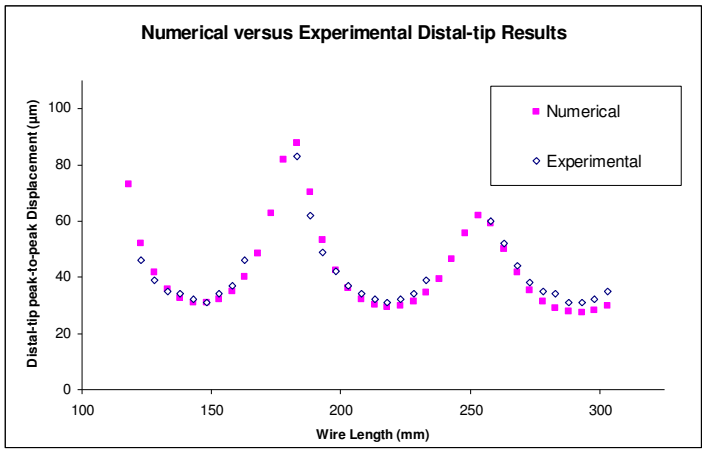

Figure 7: Comparison of numerical and experimental distal tip results for multiple waveguide lengths (no ball-tip)

Analytical Lengths (mm)	Experimental Lengths (mm)	Percentage Error (%)
144.8 (n=4)	*143*	*1.24*
217.2 (n=6)	*218*	*0.36*
289.6 (n=8)	*288*	*0.55*

Table 2: Comparison of experimental and analytical non-resonant lengths

3.2 Fluid Results

Figure 6 shows the effect the presence of ball-tip and surrounding fluid has on the resonant frequencies of the waveguide. The effect is moderate as only a small mass of fluid is being moved by the waveguides distal-tip. This is affected by the distal-tip amplitude, the geometry of the distal tip and also the properties of the fluid surrounding the tip.

The pressure field developed around a 1mm diameter wire waveguide with a 2.6mm diameter spherical ball-tip at 22.5 kHz is shown in Figure 8. This model is similar in geometry and properties to an apparatus described by Makin et al [19]. These authors performed experimental measurements of the pressure field axially ahead of the distal-tip. A comparison of the numerical model developed here and the experimental work in the literature is shown in Figure 9.

These results show that the model is capable of accurately determining the pressure field surrounding a vibrating ultrasonic waveguide No experimental measurements of the pressure amplitude close to the tip were recorded as this could result in damage to the hydrophone [19] but the numerical results show that in the region close to the tip pressure amplitudes greater than 800kPa are predicted for this arrangement. These values are capable of causing cavitation at the frequencies modelled.

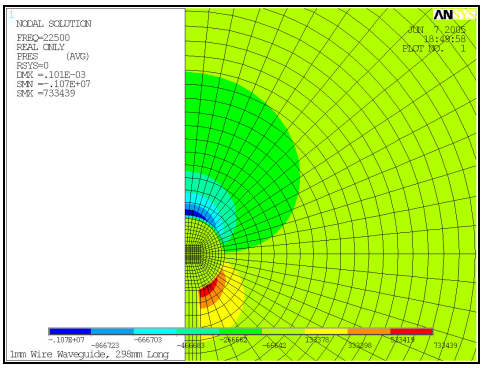

Figure 8: Pressure field developed around 2.6mm diameter distal ball-tip with displacement amplitude of 100µm

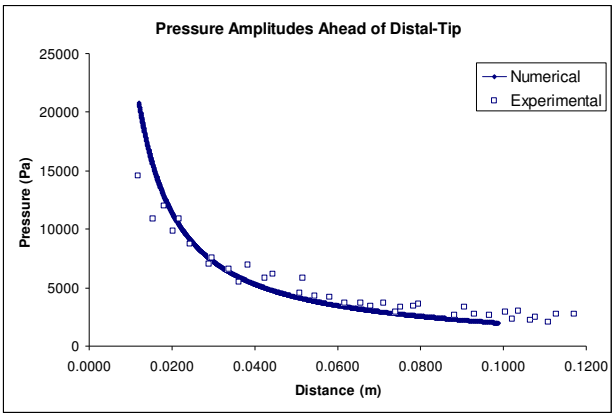

Figure 9: Comparison of numerical pressure field results and those determined experimentally by Makin et al [19]

4 CONCLUSIONS

The coupled acoustic numerical model discussed can be used to predict the behaviour of an ultrasonic wire waveguide and how it affects surrounding fluids such as blood. The structural results show the resonant frequencies of the waveguide and how varying lengths of waveguide when driven at a constant frequency can greatly affect the distal-tip displacement values. These results have been validated against an experimental wire waveguide apparatus operating at 23.5 kHz.

The numerical results from the surrounding fluid show that a dipole-like pressure field is developed around the distal-tip due to the ultrasonic vibration. This decays monotonically with distance. A numerical model similar to an experimentally tested apparatus described by Makin [19] showed good comparison and can further predict that in the region close to the distal-tip pressure amplitudes are sufficient to cause cavitation at the operational frequency. This model will prove a valuable design tool in the further investigation of this method of ultrasonic delivery in cardiovascular surgery.

ACKNOWLEGDEMENTS

This work was funded by Enterprise Ireland and Medtronic Vascular, Ireland under an Innovation Partnership Agreement.

REFERENCES

[1] American Heart Association, *International Cardiovascular Disease Statistics, Update, www.americanheart.org*, 2004.

[2] World Health Organization, *World Health Report Publications, www.who.int/cardiovascular_diseases/en*, 2004.

[3] Salunke N.V. and Topoleski L.D.T., Biomechanics of Atherosclerotic Plaque, *Critical Reviews in Biomedical Engineering*, 25(3), pp. 243- 285, 1997.

[4] Ariani M., Fishbein M.C., Chae J.S., Sadeghi H., Don Michael T.A., Dubin S.B., Siegel R.J., Dissolution of Peripheral Arterial Thrombi by Ultrasound, *Circulation*, 84, pp. 1680-1688, 1991.

[5] Folland ED, Chapter 1: Balloon Angioplasty, *In: Current Review of Interventional Cardiology. Topol E.J., Serruys P.W. (eds.)*, Philadelphia, 1994.

[6] William N.G., Chen W., Lee P., Lau C., Initial experience and safety in the treatment of chronic total coronary occlusions with a new optical coherent reflectometry-guided radiofrequency ablation guidewire, *The American Journal of Cardiology*, 92(6), pp. 732-734, 2003.

[7] Loree H.M., Grodzinsky A.J., Park S.Y., Gibsom L.J., Lee R.T., Static Circumferential Tangential Modulus of Human Atherosclerotic Tissue, *J. Biomech*, 27(2), pp. 195-204, 1994.

[8] Topoleski L.D.T., Salunke N.V., Humphrey J.D., Mergner W.J, Composition and history-dependent radial compressive behavior of human atherosclerotic plaque, *J. Biomed. Mater. Res*, 35, pp. 117- 127, 1997.

[9] Topoleski L.D.T. and Salunke N.V., Mechanical behavior of calcified plaques: a summary of compression and stress-relaxation experiments, *Z Kardiol*, 89(2), pp. 85- 91, Steinkopff Verlag, 2000.

[10] Moussa I., Di Mario C., Moses J., Reimers B., Di Francesco L., Martini G., Tobis J., Colombo A., Coronary stenting after rotational atherectomy in calcified and complex lesions: angiographic and clinical follow-up results, *Circulation*, 96, pp. 128- 136, 1997.

[11] Yock P.G. and Fitzgerald P.J., Catheter-based ultrasound thrombolysis: Shake, rattle and reperfuse, *Circulation*, 95, pp. 1360- 1362, 1997.

[12] Sobbe A., Stumpff U., Trubenstein G., Figge H., Kozuschek W., Die Ultraschall-Auflosung von Thromben, *Klin Wochenschr*, 52, pp. 1117- 1121, 1974.

[13] Siegel R.J., Fishbein M.C., Forrester J., Moore K., DeCastro E., Daykhovsky Z., Don Michael T.A., Ultrasonic Plaque Ablation: a new method for recanalisation of partially or totally occluded arteries, *Circulation*, 78: pp. 1443- 1448, 1988.

[14] Rosenschien U., Bernstein J., Di Segni E., Kaplinsky E., Bernheim J., Rozenszain L.A., Experimental Ultrasonic angioplasty: disruption of atherosclerotic plaques and thrombi in vitro and arterial recanalisation in vivo, *J Am Coll Cardiol*, 15, pp. 711- 717, 1990.

[15] Atar S., Luo H., Nagai T., Siegel R.J., Ultrasonic Thrombolysis: catheter-delivered and transcutaneous applications, *European Journal of Ultrasound*, 9, pp. 39-54, 1999.

[16] Demer L.L., Mehrdad A., Seigel R.J., High Intensity Ultrasound Increases Distensibility of Calcific Atherosclerotic Arteries, *JACC*, 18(5), pp. 1259-62, 1991.

[17] Siegel R.J., Use of Therapeutic Ultrasound in Percuntaneous Coronary Angioplasty, experimental In Vitro studies and Initial Clinical Experience, *Circulation*, 89(4), 1994.

[18] Gavin G.P., G.B. McGuinness, F. Dolan, M.S.J. Hashmi, Development and Performance Characteristics of an Ultrasound Angioplasty Device, *Proc. 11th Ann. Conf. BioEng. R. Accad. Med.*, Dublin, Ireland, pp. 78, 2005.

[19] Makin I. and Everback E.C., Measurement of pressure and assessment of cavitation for a 22.5 kHz intra-arterial angioplasty device, *J. Acoust. Soc. Am.*, 100(3), pp. 1855- 1864, 1996.

[20] Robert F. Steidel Jr., *An Introduction to Mechanical Vibrations, 3rd Edition*, Wiley, 1989.